



5 **Supplementary Note 1: Modelling of the reaction dynamics**

6 We perform model calculations to describe in more detail the measured dynamics of the atom/  
7 molecule system, triggered by the initial heat pulse. For this, we integrate the following coupled  
8 system of rate equations for the atom number  $N_A$ , the molecule number  $N_M$  and the temperature  
9  $T$ ,

$$\dot{N}_A = C_2 a_1 \frac{N_M^2}{\sigma_r^2 \sigma_{ax}} - R_2 a_2 \frac{N_M N_A^2}{\sigma_r^4 \sigma_{ax}^2} \quad (1)$$

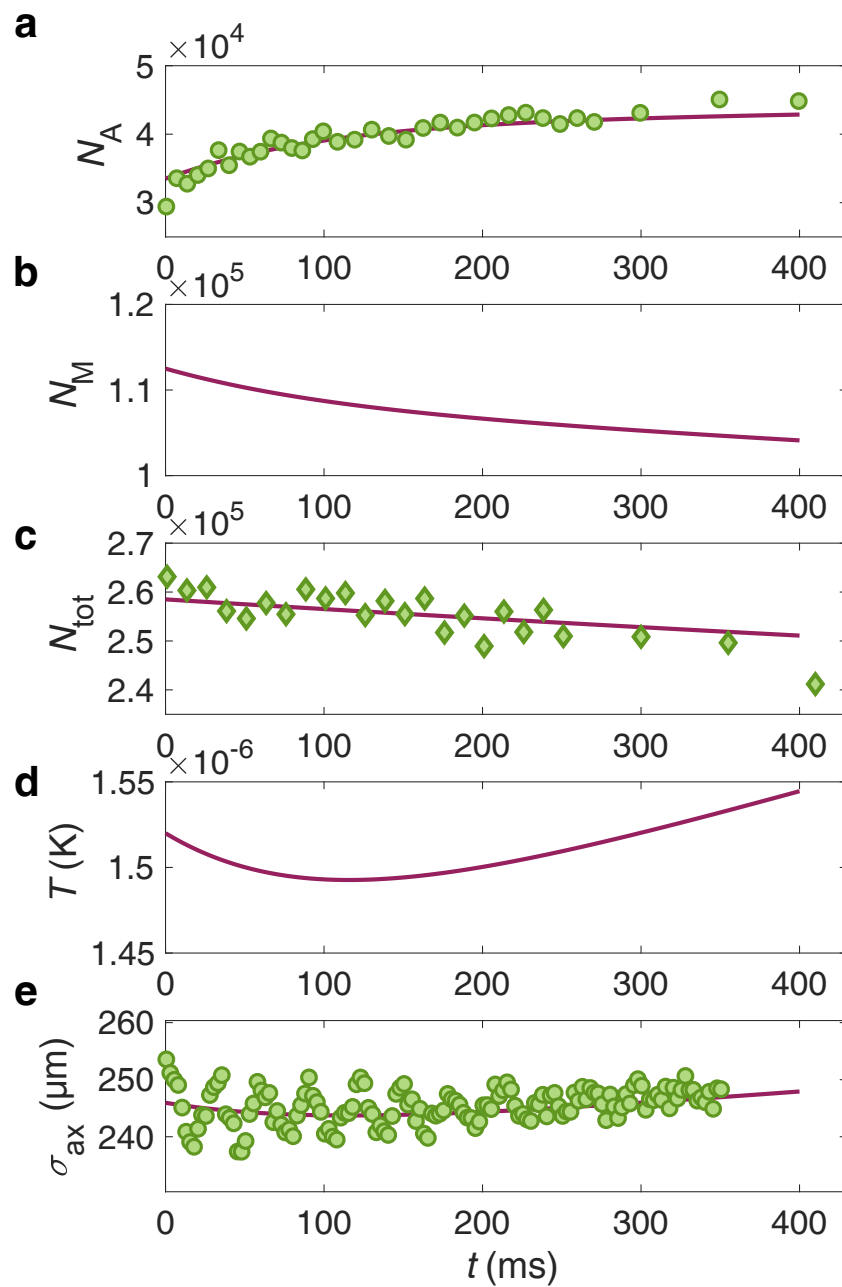
$$\dot{N}_M = -\frac{\dot{N}_A}{2} - C_{DD} a_1 \frac{N_M^2}{2 \sigma_r^2 \sigma_{ax}} \quad (2)$$

$$\dot{T} = -\frac{E_b}{6k_B (N_A + N_M)} \dot{N}_A + C_H \quad (3)$$

12 where  $a_1 = (4\pi^{3/2})^{-1}$  and  $a_2 = 2^{-7}(2\pi^2)^{-3/2}$  are numerical constants. Equation (1) is identical  
13 to eq. (2) in the main text. The first term in eq. (2) corresponds to the conversion between  
14 molecules and unbound atoms, while the second term accounts for molecule losses in inelastic  
15 dimer-dimer collisions with rate constant of  $C_{DD} = 2.3 \times 10^{-13} \text{ cm}^3 \text{ s}^{-1}$ , which is extracted from  
16 the previous measurement of ref.<sup>1</sup>. Equation (3) has two contributions. The first one accounts  
17 for cooling due to endothermic dissociation and heating due to exothermic recombination reac-  
18 tions. The second contribution corresponds to background heating of the gas caused, e.g., by  
19 off-resonant scattering of the dipole-trap light. Equations (1) and (2) are coupled via the cloud  
20 sizes  $\sigma_{r(ax)} = \sqrt{k_B T / m_M \omega_{r(ax)}^2}$  to the temperature equation (3).

21 The results of a corresponding calculation at 709 G are shown in Supplementary Fig. 1 and are  
22 in very good agreement with the experimental data. The values of the parameters  $C_2$  and  $R_2$  are  
23 the same as in the main text.  $C_H = (3.0 \pm 1.0) \times 10^{-7} \text{ s}^{-1}$  is mainly determined by the long-time  
24 evolution of the cloud size (see Supplementary Fig. 1d,e).

25 The total particle number in Supplementary Fig. 1c) exhibits the losses caused by the inelastic  
26 dimer-dimer collisions and agrees well with the experimental measurements. The temperature in  
27 Supplementary Fig. 1d) first decreases slightly due to endothermic dissociation after the heat pulse  
28 and then increases again due to the dipole-laser induced photodissociation. Supplementary fig. 1e  
29 shows the calculated cloud width  $\sigma_{ax}$  as determined by the temperature  $T$ . It agrees well with the  
30 measurements (green circles) if we average over the small-amplitude collective oscillations which  
31 have been excited by the initial heat pulse.  
32



Supplementary Figure 1. Model calculation for the evolution of the atom/ molecule system. Results from the coupled differential equations (1-3) (continuous lines). Plot symbols show experimental data for 709G. For details see text of Supplementary Note 1.

33

### Supplementary Note 2: Thermometry

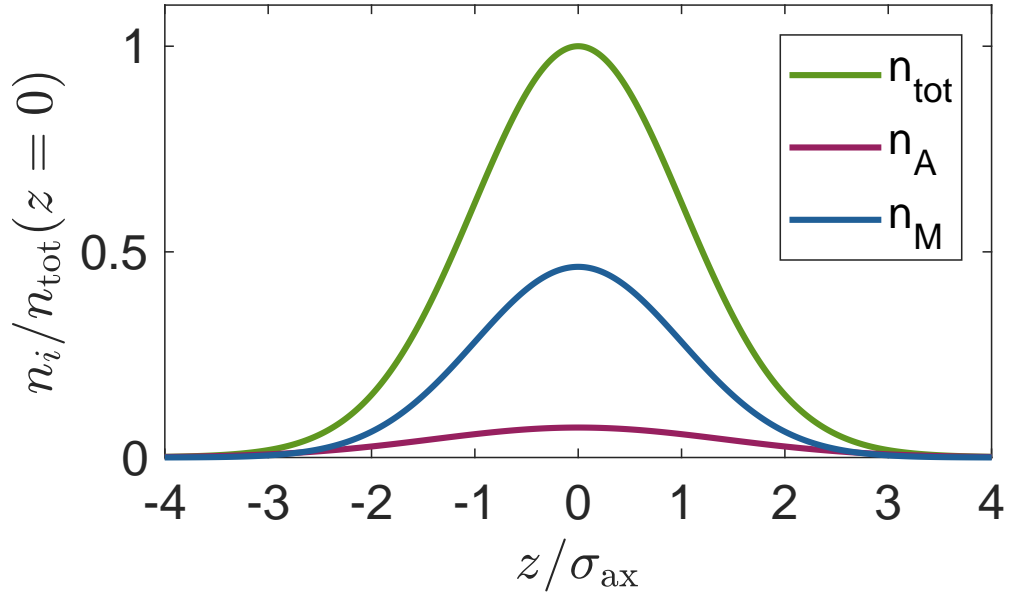
34 Within the parameter range of our experiments the molecular and atomic density distributions  
 35 are each well described by that of a non-interacting thermal gas located in a harmonic trap. The

36 axial sizes of the molecular and atomic clouds are given by  $\sigma_{ax} = \sqrt{k_B T / m \omega_{ax}^2}$  and  $\sigma_{ax,A} =$   
 37  $\sqrt{2} \sigma_{ax}$ , respectively. Because the axial trapping frequency  $\omega_{ax}$  is precisely known for our setup,  
 38 we can determine the temperature  $T$  by measuring the molecular or atomic cloud size. These cloud  
 39 sizes are extracted from images of the mixed atom/ molecule clouds after careful analysis, for  
 40 which we also determine the atom fraction  $N_A / N_{tot}$  of the cloud. Supplementary Figure 2 shows  
 41 a calculated typical example for the 1D density distributions (where the transverse directions have  
 42 been integrated out) for atoms  $n_A$ , molecules  $n_M$  and both  $n_{tot} = 2n_M + n_A$ .

### 43 Supplementary Note 3: Rescaling the measured $C_2$ to a constant temperature

44 Supplementary table 1 is the list of temperatures at which the  $C_2$  measurements in fig. 3c are  
 45 taken. The statistical uncertainty of the temperatures is around  $\Delta T = 0.08 \mu\text{K}$ .

46 The temperatures increase with decreasing scattering length  $a$ . This temperature change is  
 47 a result of the way we prepare the sample. In particular, the magnetic field ramp to the target  
 48 field takes place within a  $21 \mu\text{K} \times k_B$  deep trap which prevents further evaporative cooling. With



Supplementary Figure 2. Calculated 1D density distribution for a thermal cloud of atoms and molecules. In a harmonic potential non-interacting atoms and molecules exhibit a Gaussian density distributions  $n_A$  and  $n_M$ , respectively, of which the widths differ by a factor of  $\sqrt{2}$ . The total density distribution is the sum  $n_{tot} = 2n_M + n_A$ . Here, the atom fraction  $N_A / N_{tot}$  is 0.6.

Supplementary Table 1. Temperatures and scattering lengths of the measurements in fig. 3c.

$a$ ( $a_0$ )	1760	1830	1920	2000	2090	2180	2280
$T$ ( $\mu\text{K}$ )	1.60	1.52	1.51	1.47	1.42	1.41	1.35

49 decreasing  $a$ , the binding energy of the dimers increases and therefore for a given temperature the  
 50 equilibrium molecule fraction increases. The corresponding molecular association, however, heats  
 51 the sample.

52

**SUPPLEMENTARY REFERENCES**

- 53 <sup>1</sup> Bourdel, T. et al. Experimental Study of the BEC-BCS Crossover Region in Lithium 6. *Phys. Rev. Lett.*  
54 **93**, 050401 (2004).